International Journal of Engineering Research and Application www.ijera.com ISSN : 2248-9622 Vol. 8,Issue 12 (Part -III) Dec 2018, pp 81-86

RESEARCH ARTICLE OPEN ACCESS

A Novel Control Strategy for Hybrid Ac/Dc Micro Grid Systems

Sushree Shataroopa Mohapatra[1] , Anjushree Behera[2], Sibananda Mishra[3]
[1,3]*Assistant Professor,Dept. of electrical & electronics engineering ,Gandhi Institute for Technology Bhubaneswar,India*
[2]*Assistant Professor,Dept. of electrical & electronics engineering Gandhi Engineering College,Bhubaneswar,India*

ABSTRACT: The smart grid design aims to provide overall power system monitoring, protection and control strategies to maintain system performance, stability and security. This paper develops control strategies for smart hybrid micro grid systems. A hybrid AC/DC micro grid is simulated and integrated to the AC system with appropriate control capability. The converter control strategies for grid connected and islanding mode are presented. A real-time energy management algorithm in hybrid micro grid systems is proposed to evaluate the effects of using energy storage resources and their use in mitigating heavy load impacts on system stability and operational security. MATLAB/SIMULINK is used to create and simulate the proposed system.
Key words: Hybrid power systems, micro grid, power management strategies, smart grid.

I. INTRODUCTION

The smart grid concept is currently prevailing in the electric power industry [1-5]. The objective of constructing a smart grid is to provide reliable, high quality electric power to digital societies in an environmentally friendly and sustainable way. The dc micro grid has been proposed [6]–[7] to integrate various distributed generators. One of most important futures of a smart grid is the advanced structure which can facilitate the connections of various ac and dc generation systems, energy storage options, and various ac and dc loads with the optimal asset utilization and operation efficiency. To achieve these goals, power electronics technology plays a most important role to interface different sources and loads to a smart grid. A hybrid ac/dc micro grid is proposed in this paper to reduce processes of multiple reverse conversions in an individual acor dc grid and to facilitate the connection of various renewable ac and dc sources and loads to power system. Since energy management, control, and operation of a hybrid grid are more complicated than those of an individualac or dc grid, different operating modes of a hybrid ac/dc grid have been investigated. The coordination control schemes among various converters have been proposed to harness maximum power from renewable power sources, to minimize power transfer between ac and dc networks, and to maintain the stable operation of both ac and dc grids under variable supply and demand conditions when the hybrid grid operates in both grid-tied and islandingmodes.

II. MODELING OFCOMPONENETS

A. Modeling of PVPanel:

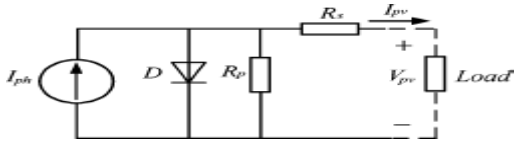

Fig. 1. Equivalent circuit of a solar cell

Fig 1 shows the equivalent circuit of a PV panel with a load. The current output of the PV panel is modeled by the following threeequations.

$$I_{pv} = n_p I_{ph} - n_p I_{sat} \times \left[\exp\left(\left(\frac{q}{AkT}\right)\left(\frac{V_{pv}}{n_s} + I_{pv}R_s\right)\right) - 1\right] \quad (1)$$

$$I_{ph} = \left(I_{sso} + k_i\,(T - T_r)\right).\frac{S}{1000} \quad (2)$$

$$I_{sat} = I_{rr}\left(\frac{T}{T_r}\right)^3 \exp\left(\left(\frac{qE_{gap}}{kA}\right).\left(\frac{1}{T_r} - \frac{1}{T}\right)\right) \quad (3)$$

B. Modeling of Battery:
Two important parameters to represent state of a battery are terminal voltage v_b and state of charge (SOC) as follows

$$V_b = V_0 + R_b.i_b - K\frac{Q}{Q + \int i_b dt} + A.\exp(B\int i_b dt) \quad (4)$$

SOC= 100 (5)

inductance, is the flux linkage, u and i

represent voltage and current respectively,ω1 and ω2 are the angular synchronous speed and slip speed respectively, ω2 = ω1- ωr ,Tm is the mechanical torque, Tem is the electromagnetic torque.

Where Rb is internal resistance of the battery, Vo is the open circuit voltage of the battery, ib is battery charging current, K is polarization voltage, Q is battery capacity, A is exponential voltage, B and is exponentialcapacity.

C. Modeling of Wind TurbineGenerator:

Power output Pm from a Wind Turbine Generator (WTG) is determined by (6)

$$P_m = 0.5\,\rho\, A C_p\,(\lambda,\beta) V_w^3 \quad (6)$$

Where ρ is air density, A is rotor swept area, Vω is wind speed, and $C_p\,(\lambda,\beta)$is the power coefficient, which is the function of tip speed ratio and pitch angleβ.The mathematical models of a double fed induction generator (DFIG) are essential requirement for its control system. The voltage equations of an induction motor in a rotating d-q coordinate are as follows:

$$\begin{bmatrix} u_{ds} \\ u_{qs} \\ u_{dr} \\ u_{qr} \end{bmatrix} = \begin{bmatrix} -R_s & 0 & 0 & 0 \\ 0 & -R_s & 0 & 0 \\ 0 & 0 & R_r & 0 \\ 0 & 0 & 0 & R_r \end{bmatrix} \begin{bmatrix} i_{ds} \\ i_{qs} \\ i_{dr} \\ i_{qr} \end{bmatrix} + p \begin{bmatrix} \lambda_{ds} \\ \lambda_{qs} \\ \lambda_{dr} \\ \lambda_{qr} \end{bmatrix} + \begin{bmatrix} -\omega_1 \lambda_{qs} \\ \omega_1 \lambda_{ds} \\ -\omega_2 \lambda_{qr} \\ \omega_2 \lambda_{dr} \end{bmatrix} \quad (7)$$

$$\begin{bmatrix} \lambda_{ds} \\ \lambda_{qs} \\ \lambda_{dr} \\ \lambda_{qr} \end{bmatrix} = \begin{bmatrix} -L_s & 0 & L_m & 0 \\ 0 & -L_s & 0 & L_m \\ -L_m & 0 & L_r & 0 \\ 0 & -L_m & 0 & L_r \end{bmatrix} \begin{bmatrix} i_{ds} \\ i_{qs} \\ i_{dr} \\ i_{qr} \end{bmatrix} \quad (8)$$

The dynamic equation of the DFIG

$$\frac{J}{n_p}\frac{d\omega_r}{dt} = T_m - T_{em} \quad (9)$$

$$T_{em} = n_p L_m (i_{qs} i_{dr} - i_{ds} i_{qr}) \quad (10)$$

Vector equations in the stator voltage oriented reference frame are

$$i_{ds} = -\frac{L_m}{L_s} i_{dr} \quad T_{em} = n_p \frac{L_m}{L_s} \lambda_s i_{dr} \quad \sigma = \frac{L_s L_r - L_m^2}{L_s L_r} \quad (11)$$

$$u_{dr} = R_r i_{dr} + \sigma L_r \frac{d i_{dr}}{dt} - (\omega_l - \omega_r)(L_m i_{qs} + L_r i_{qr}) \quad (12)$$

$$u_{qr} = R_r i_{qr} + \sigma L_r \frac{d i_{qr}}{dt} + (\omega_l - \omega_r)(L_m i_{ds} + L_r i_{dr}) \quad (13)$$

III. CONTROLSTRATEGIES

A. Grid connectedMode

Block diagram of boost converter and main converter is given in Fig.2.

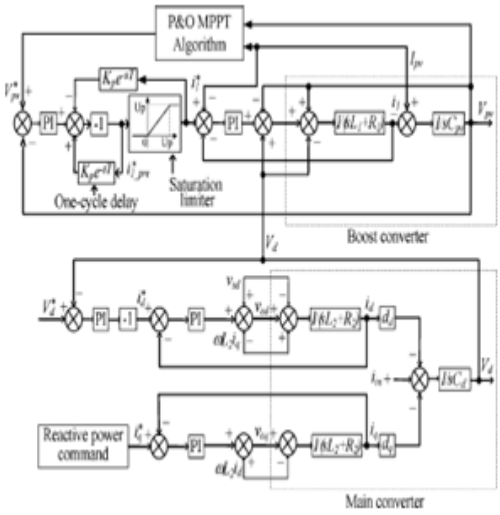

Fig. 2. Block diagram of boost converter and main converter.

The reference value of the solar panel terminal voltage is determined by the basic perturbation and observation (P&O) algorithm based on solar irradiation and temperature to harness the maximum power. Dual-loop control scheme is applied for the PV system to track optimal solar power .The outer voltage loop guarantee reference voltage tracking with zero steady-state error and the inner current loop can improve dynamic response. Two PI controllers are used for real and reactive powercontrol

Where the subscripts d, q ,s, and denote d-axis, q- axis, stator, and rotor respectively, L represents the respectively. When resource conditions or load capacities change, the dc bus voltage is adjusted to constant through PI regulation. The PI controller is set as instantaneous active current id reference whereas the instantaneous reactive current iq reference is determined by reactive power compensationcomm and. The rotor rotational speed is obtained through the maximum power point tracking (MPPT) algorithm, which is based on the power and speed characteristic of the wind turbine. The rotational speed and mechanical power are used to calculate the electromagnetic torque . Axis rotor side current reference is determinedbased onT_{em}^* through stator flux estimation. The rotor side d-q voltages are maintained through controlling the corresponding current with appropriate feed forward voltage compensation. The direct torque control logic diagram is shown in Fig.3.

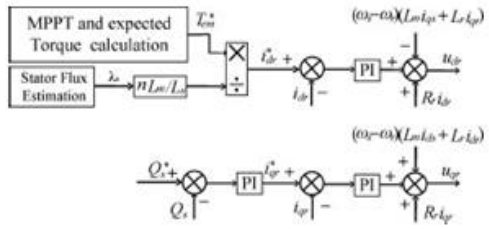

Fig. 3. The direct torque control scheme for the rotor side converter

B. IsolatedMode:

When the hybrid grid operates in the islanding mode, the boost converter and the back-to-back ac/dc/ac converter of the DFIG may operate in the on-MPPT or off-MPPT based on system power balance and energy constraints. The main converter acts as a voltage source to provide a stable voltage and frequency for the ac grid and operates either in inverter or converter mode for the smooth power exchange between ac and dc links. The battery converter operates either in charging or discharging mode based on power balance in the system. The dc- link voltage is maintained by either the battery or the boost converter based on system operating condition. Powers under various load and supply conditions should be balanced asfollows: based on the systemnet power$P_{net}$and the energy constraints and the charging/discharging rate of battery. The energy constraints of the battery are determined based on the state of charge (SOC) limits using $SOC_{min} < SOC \leq SOC_{max}$.fromFig.4.

The constraint of charging and dischargingrateis$P_b \leq P_{bmax}$. At local level, the individual converters operate based on mode commends from the EMS. The battery converter may operate in theidle,
charging, or discharging mode for different cases. The main converter will operate in the inverter mode if P_{acL}) is negative or in the converter mode withpositive). Load shedding is required to maintain power balance if power supply is less than demand and the battery is at the minimumSOC.

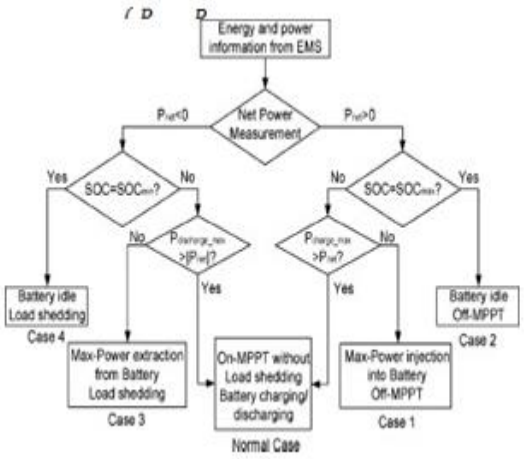

Fig.4. Control mode diagram for the isolated hybrid grid

$$P_{pv} + P_w = P_{acL} + P_{dcL} + P_{loss} + P_b$$

Where is the total gridlosses
(14)

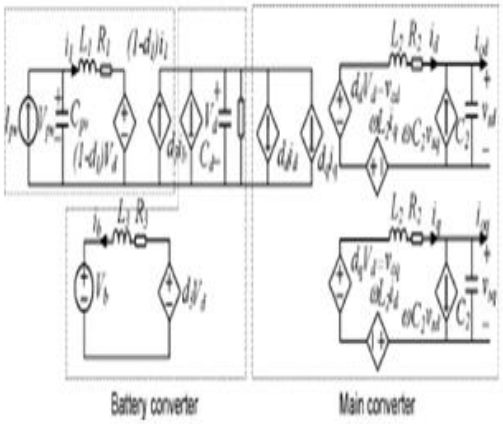

Fig.5. Time average equivalent circuit model for threeconverters.

$$P_{pv} + P_w = P_{acL} + P_{dcL} + P_{loss} + P_b \qquad (14)$$

Where P_{loss} is the total gridlosses

Two level coordination controls are used to maintain system stable operation. At the system level, operation modes of the individual converters are determined by the energy management system (EMS) The time average equivalent circuit model of the booster, main converter, and battery converter for the isolated operation is shown in Fig5. The current and voltage equations for the battery converter and dc link are asfollows:

$$V_D - V_b = L_3.\frac{di_b}{dt} + R_3 i_b \quad (15)$$

$$V_D = V_d.d_3 \quad (16)$$

$$i_1(1-d_1) - i_{ac} - i_{dc} - i_b.d_3 = i_c = C_d.\frac{dV_d}{dt} \quad (17)$$

Where $d_3$and $(1-d_3)$are the duty ratio of the switches ST_7andST_8respectively.

The ac side current equations of the main converter in
d-q coordinate are as follows:

$$C_2\frac{d}{dt}\begin{bmatrix}v_{sd}\\v_{sq}\end{bmatrix}=\begin{bmatrix}i_d\\i_q\end{bmatrix}+\begin{bmatrix}0 & \omega\\-\omega & 0\end{bmatrix}\begin{bmatrix}v_{sd}\\v_{sq}\end{bmatrix}-\begin{bmatrix}i_{vd}\\i_{vq}\end{bmatrix} \quad (18)$$

Where $i_{vd}$and $i_{vq}$are d-q currents at the converter side of the transformerrespectively. To provide a stable dc-link voltage, the dual loop control scheme is applied for the battery converter. The injection current I_{in}givenas
$I_{in} = i_1(1-d_1) - i_{ac} - i_{dc}$.

It should be noted that the output of the outer voltage loop is multiplied by(-1) before it is set as the inner loop current reference. Current $i_{b1}$is defined positive when flowing into the battery, where the preset dc- link voltage V_{dc}^* is set to constant 400 V. Thebattery converter is transferred from discharging into charging mode in this control method. The main converter provides a stable ac bus voltage for the DFIG converter as shown in the bottom of Fig.6

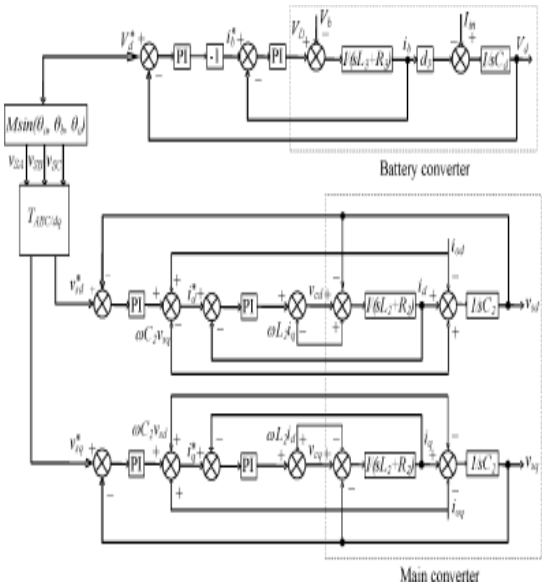

Fig.6. Block diagram of the battery and main converters for the normal case

The coordinated control block diagram for the normal case is shown in Fig. 7. The control objectives for the converters change when the system transfers from one operating scenario to another. The boost converter provides a stable dc-link voltage. The main converter is controlled to provide a stable ac bus voltage. The current $I_0$is equal to $i_{ac} + i_{dc} + i_b d_3$
and $d_{11}$is equal to $(1-d_1)$.

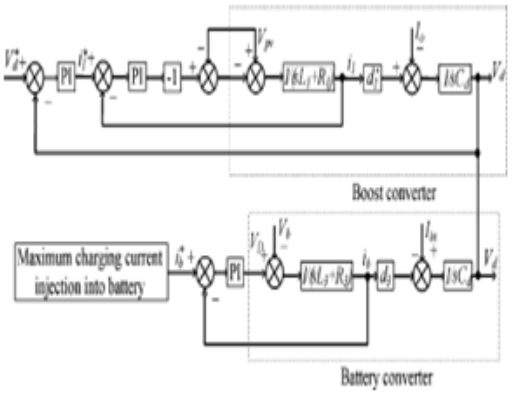

Fig.7. Block diagram of the booster and battery converter for Case 1

The anti-islanding technique is one of the essential functions for reliable operation of distributed generation systems [8-10]. Many anti-islanding detection and control schemes have been developed for conventional and power-converter-based distributed generators and various micro grids [11].

IV. SIMULATION RESULTS

The operations of the hybrid under various sources and load conditions are simulated by using Matlab and verified the proposed control algorithms. The simulation results are presented in two cases with grid connected mode and isolatedmode.

Case (i): Grid connected Mode:

In case of grid connected mode the main converter operates in the PQ mode. Power is balanced by the utility grid. The battery is fully charged and operates in the rest mode in the simulation. The AC bus voltage is maintained by the utility grid and DC bus voltage is maintained by the main converter. The optimal terminal voltage is determined using the basic P&O algorithm based on the corresponding solarirradiation. Figure 8 shows the voltage (0.2 times voltage for comparison) and current response at the AC side of the main converter when the solar irradiation level decreases from 1000W/ m^2at 0.3seconds to 400W/ at 0.4seconds with a fixed DC load 20KW.

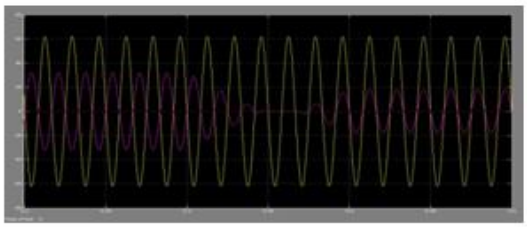

Fig.8. Ac side voltage and current of the main converter with variable solar irradiation level and constant DCload

Figure 9 shows the current directions that the power is injected from the DC to the Ac grid before 0.3 seconds and reversed after 0.4 seconds. It can be seen from the current direction that the power is injected from DC to AC grid before 0.25seconds and reversed after0.25seconds

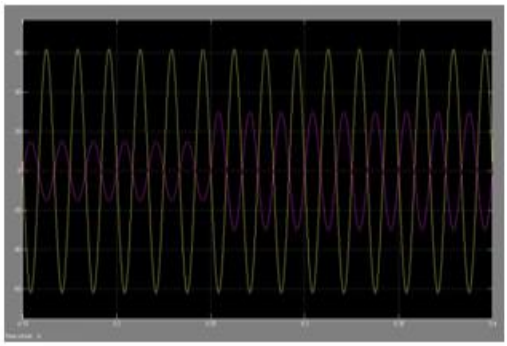

Fig.9. Ac side voltage and current of the main converter with constant solar irradiation level and variable DCload

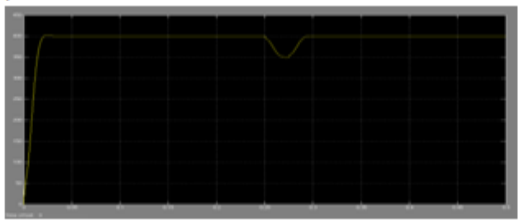

Fig.10. DC bus voltage transient response

The figure 10 shows voltage response at the DC side of the main converter under the same conditions. The figure shows that the voltage drops at 0.25 second and recovers quickly by thecontroller.

Case (ii): Isolated Mode:
In case of isolated mode the control strategies are presented in two cases. Under this two cases are considered.

(i) NormalMode:

In the normal case, DC bus voltage is maintained stable by the battery converter and AC bus voltage is provided by the main converter. The reference of DC
- link voltage is set as 400volts.
Figures 11&12 show simulation output for output power of the DFIG, and AC side voltage VS current (voltage times 1/3 for compression). It is observed thattheACgridinjectspowertotheDCgridbefore 0.3 seconds and receives power from the DC grid after 0.3 seconds. The voltage at the Ac bus is kept 326.5 volts constant regard less of load conditions. The nominal voltage and rated capacity of the battery are selected as 200 volts and 65Ah respectively.

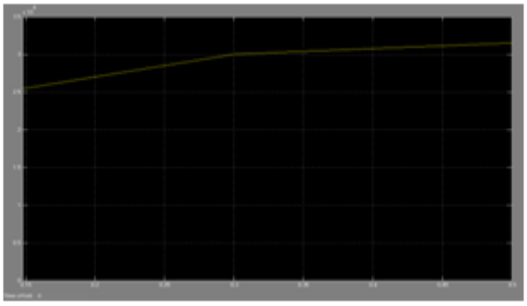

Fig. 11. Output power of the DFIG

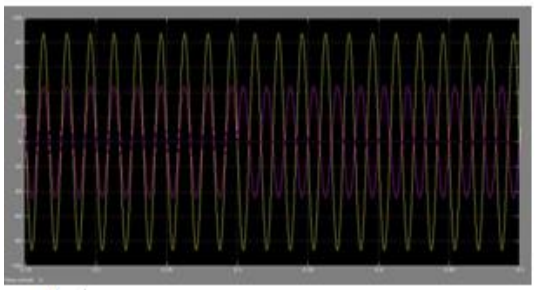

Fig. 12. AC side voltage VS current (voltage times 1/3 for compression)

The fig. 13 shows the transient process of the DFIG power output, which becomes stable after 0.45 seconds due to the mechanical inertia.

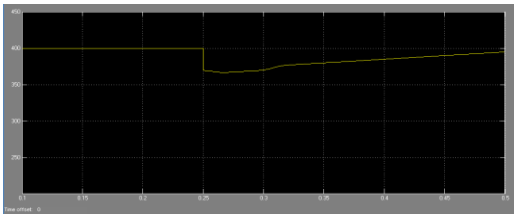

Fig 13. DC bus voltage transient response in isolated mode.

(ii) MPPT offmode:

Figure 14 shows that the total power generated is greater than the total load before 0.3 seconds and less than the total load after 0.3 seconds, and the voltage drops at 0.3 seconds and recovers to 40 volts quickly when the system is at off MPPT mode.

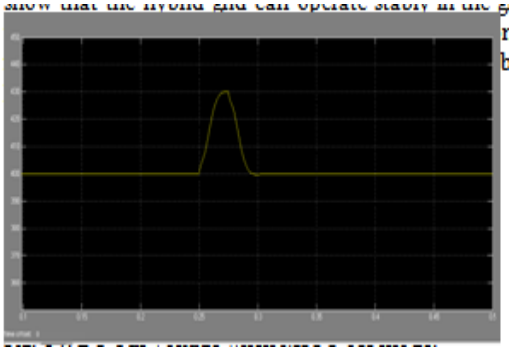

Fig. 14. DC bus voltage when MPPT off mode.

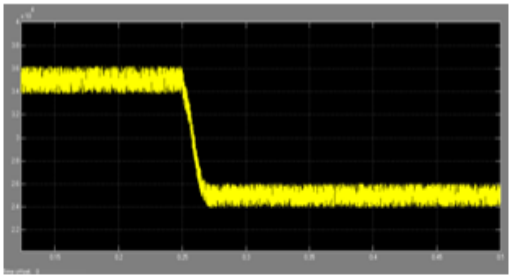

Fig. 15. PV output when MPPT off mode

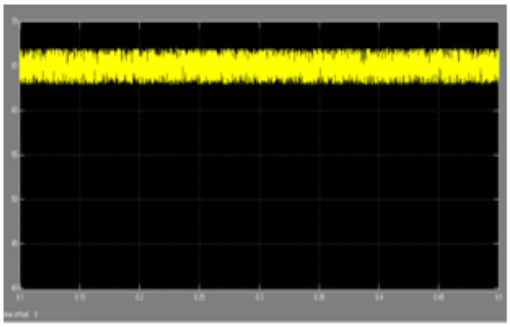

Fig. 16. Battery current when MPPT off mode

The figures 15and 16 show PV output power, and battery charging current respectively when the dc load decreases from 20kW to 10kW at 0.2s with a constant solar irradiation level 1000W/m2. The battery discharging current is kept constant at 65A. The dc bus voltage is stabilized to 400V after 0.005s from the load change. The PV power output drops from the maximum value after 0.2s, which means that the operating modes are changed from MPPT to off-MPPT mode. The PV output power changes from 35kW to 25kW after0.2s.

V. CONCLUSION

Different source conditions and load capacities are tested to validate the control methods. The simulation results show that the hybrid grid can operate stably in the grid-tied and in isolated mode also. Stable ac and dc bus voltage can be guaranteed when the operating conditions or load capacities change in the two modes. The power is smoothly transferred under varying load conditions between storage and PV Sources.

REFERENCE

[1]. R. H. Lasseter, "Micro Grids," in Proc. IEEE Power Eng. Soc. Winter Meet., Jan. 2002, vol. 1, pp.305–308.

[2]. Y. Zoka, H. Sasaki, N. Yorino, K. Kawahara, and C. C. Liu, "An interaction problem of distributed generators installed in a Micro Grid," in Proc. IEEE Elect. Utility Deregulation, Restructuring. Power Technol., Apr. 2004, vol. 2, pp.795–799.

[3]. R. H. Lasseter and P. Paigi, "Micro grid: A conceptual solution," in Proc. IEEE 35th PESC, Jun. 2004, vol. 6, pp. 4285–4290.

[4]. C. K. Sao and P. W. Lehn, "Control and power management of converter fed Micro Grids," IEEE Trans. Power Syst., vol. 23, no. 3, pp. 1088–1098, Aug.2008.

[5]. T. Logenthiran, D. Srinivasan, and D.Wong, "Multi- agent coordination for DER in Micro Grid," in Proc. IEEE Int. Conf. Sustainable Energy Technol., Nov. 2008, pp. 77– 82.

[6]. M. E. Baran and N. R. Mahajan, "DC distribution for industrial systems: Opportunities and challenges," IEEE Trans. Ind. Appl., vol. 39, no. 6, pp. 1596–1601, Nov. 2003.

[7]. Y. Ito, Z.Yang, and H. Akagi, "DC micro-grid based distribution power generation system," in Proc. IEEE Int. Power Electron. Motion Control Conf., Aug. 2004, vol. 3, pp. 1740–1745.

[8]. A. Sannino, G. Postiglione, and M. H. J. Bollen, "Feasibility of a DC network for commercial facilities," IEEE Trans. Ind. Appl., vol. 39, no. 5, pp. 1409–1507, Sep. 2003.

[9]. D. J. Hammerstrom, "AC versus DC distribution systems-did we get it right?," in Proc. IEEE Power Eng. Soc. Gen. Meet., Jun. 2007, pp.1–5.

[10]. D. Salomonsson and A. Sannino, "stable operation of grid with renewable energy sources in anti-islanding," IEEE Trans. Power Del., vol. 22, no. 3, pp. 1620–1627, Jul. 2007.

[11]. M. E. Ropp and S. Gonzalez, "Development of a MATLAB/Simulink model of a single-phase grid- connected photovoltaic system," IEEE Trans. Energy Conv., vol. 24, no. 1, pp. 195–202, Mar.2009.